

*V.M. Zemlyansky, Doctor of Physical and Mathematical Sciences,
M.O. Gusev, K.A. Lobzov
(National Aviation University, Ukraine)*

Laser diagnostics of hypersonic flows during testing of aircraft design

Multiwave laser Doppler anemometers are considered (MLDA)

Which can be used to measure hypersonic speeds. MLDA is based on probing by streams of pairs of laser beams, respectively, on lengths $\lambda_1, \lambda_2, \lambda_3$ formed by semiconductor lasers. The symmetrical geometry of sounding and receiving scattered radiation, the parameters of which correspond to the observation of the Zemlyansky effect [1], makes it possible to form three in-phase high-frequency signals at the same frequency at the optical mixing of the scattered radiation at the photocathode of the receiver.

The differential scheme of the laser Doppler anemometer (LDA) is widely used in aerodynamic testing of aircraft (LA) design. [2] Recently, hypersonic aircraft in many countries of the world are being tested, including flight tests. When diagnosing hypersonic flows using LDA, it is necessary to ensure a high spatial resolution of the measurement zone, which is created by the intersection of two focusable coherent laser beams at an angle γ [3]. The larger the angle γ , the smaller the size of the measurement zone. However, with an increase in the angle γ , the sensitivity of the LDA increases - $S[\text{Hz}/\text{ms}^{-1}]$.

Therefore, at air flow rates of more than 1000 ms^{-1} , the useful high-frequency signal at the photodetector output, to which scattered radiation from a high-speed air flow is directed, is in the GHz wavelength range. Since the frequency range of highly sensitive FDs is in the region up to 100 MHz, at hypersonic flow velocities, optical spectrometry is used for signal processing, which significantly reduces the accuracy of determining the frequency shift of the scattered radiation carrying information about the flow velocity.

We have developed a multi-wavelength LDA, the principle of operation is based on the four-wave mixing of $2n$ pairs of scattered beams, respectively, at wavelengths $\lambda_1, \lambda_2, \lambda_3 \dots \lambda_n$. This provides a high spatial resolution of the MLDA, and the spectrum of the useful signal lies in the 100 GHz band.

The multi-wavelength laser Doppler anemometer (BLDA) consists of (Fig. 1): "n" - the number of single-mode lasers, for example, 3 lasers 1, 2 and 3, emitting at wavelengths $\lambda_1, \lambda_2, \dots, \lambda_n$, for example bundles 4, 5 and 6; "n" - numbers of selective beam splitters for wavelengths $\lambda_1, \lambda_2, \dots, \lambda_n$ - 9, 11 and 15, which divide laser beams 4, 5 and 6 into two corresponding beams of equal intensity 9 and 10, 12 and 13, 16 and 17; "n" - the number of selective mirrors, respectively on the wavelengths $\lambda_1, \lambda_2, \dots, \lambda_n$ - 8, 14 and 18; n - the number of frequency shift devices - 19, 21 and 22, connected to the high-frequency generator 20; (n-1) - numbers of phase regulators - 23 and 25 with power supply units 24 and 26; (n+1) - numbers of

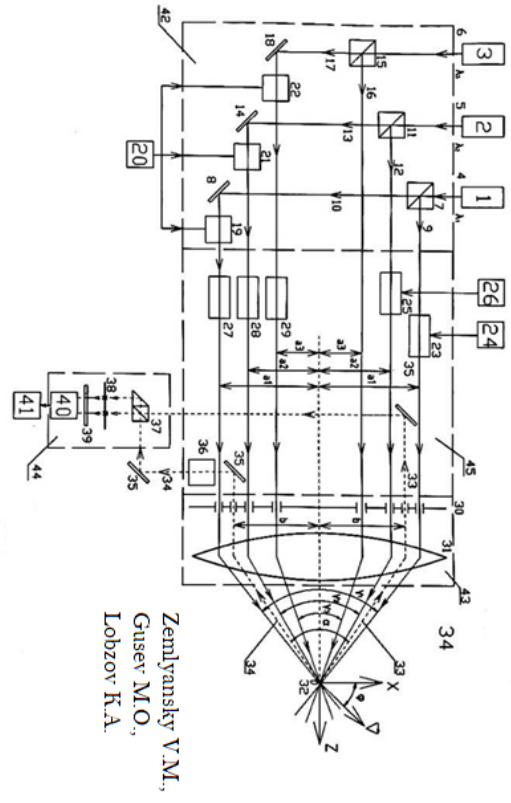
delay lines - 27, 28, 29 and 36; aperture diaphragm with $2(n+1)$ - the number of round holes - 30, focusing lens 31, measurement zone 32, in which at the angles $\gamma_1, \gamma_2, \dots, \gamma_n$ intersected by $2n$ - the number of probing beams in one OXZ plane; scattered beams 33 and 34. Multi-wave mirrors 35, multi-wave complex mixer 37, diaphragm 38 with two holes, band light filter 39, photo receiver 40, Doppler frequency meter 41; block of formation $2n$ - number of parallel beams at wavelengths $\lambda_1, \lambda_2, \dots, \lambda_n$ - 42, which includes elements and blocks: 9, 11, 15, 8, 14, 18, 19, 21 and 22; sensor 43, which includes 30, 31; optical time delay device 45, which includes: 23, 25, 27, 28, 29, 35 and 36; reception block - 44, which includes: 37, 38, 39 and 40.

BLDA works as follows. Let's consider an example of the implementation of BLDA using three lasers 1, 2 and 3. Laser 1 emits, for example, a vertically polarized beam 4 at a wavelength λ_1 , which is divided by a selective beam splitter 7 into two beams 9 and 10 of equal intensity. The beam 10 after reflection from the selective mirror 8 at the wavelength λ_1 , propagates, like beam 9, parallel and symmetrical with respect to the optical axis OZ. The second laser 2 emits a vertically polarized beam 5 at a wavelength λ_2 , which is divided by a selective beam splitter 11 into two beams 12 and 13 of equal intensity. The beam 13 after reflection from the selective mirror 14, like the beam 12, spreads symmetrically and parallel to the axis of the OZ scheme. The third laser 3 emits a vertically polarized beam 6 at a wavelength λ_3 , which is divided by a selective beam splitter 15 into two beams 16 and 17 of equal intensity. The beam 17 after reflection from the selective mirror 18 at the wavelength λ_3 , as well as beam 16, spread symmetrically and parallel to the axis of the OZ scheme.

Beams 10, 13 and 17, after passing through the corresponding frequency shift devices 19, 21 and 22, are shifted in frequency to the same fixed frequency Ω_M . Parallel beams 10, 13, and 17, after passing through the delay lines 27, 28, and 29, respectively, as well as beams 9 and 12, after passing through the phase regulators 23 and 25, respectively, and beam 16, after passing through the aperture diaphragm 30, are focused by the lens 31 in the zone measurement 32. And beams 9 and 10 at the wavelength λ_1 (Fig. 1) intersect at an angle γ_1 ; beams 12 and 13 on the wavelength λ_2 - at an angle γ_2 , and beams 16 and 17 on the wavelength λ_3 - at an angle γ_3 . Each pair of beams 9 and 10, 12 and 13, 16 and 17 has polarization matching, however, in the measurement zone 32, these pairs of beams do not interfere during their superposition, since the delay lines 27, 28 and 29, respectively, for beams 10, 13 and 17 create such a time delay $\tau_i (i=1, 2, \dots, n)$, at which the modulus of the complex degree of temporal coherence for beams 9 and 10 - $|\gamma_{12}(\tau_i)| = 0$, for beams 12 and 13 - $|\gamma_{22}(\tau_i)| = 0$, and for beams 16 and 17 - $|\gamma_{32}(\tau_i)| = 0$ (etc. for i - laser - $|\gamma_{i2}(\tau_i)| = 0$).

Beams 33 and 34 at wavelengths scattered on moving microparticles $\lambda_1, \lambda_2, \lambda_3 (\dots, \lambda_n)$, are collected at an angle α by the lens 31 within two symmetrical apertures of the diaphragm 30 (Fig. 1). Moreover, the beam 33, after reflection from the multiwave mirror 35, is directed to one input of the multiwave mixer 37, to the second input of which the scattered beam 34 is directed, after passing through the delay lines 36.

The multi-wavelength laser Doppler anemometer



Zemlyansky V.M.,
 Glusev M.O.,
 Lobzov R.A.

Fig. 1 The multi-wavelength laser Doppler anemometer

The spatially aligned beams 33 and 34 then pass through the aperture 38 of the photocathode of the photoreceiver 40. As a result of the optical mixing of scattered beams 33 and 34 at wavelengths 21, 22 and 23 (taking into account the temporal delay of the beams in the delay line 36 Such a value that $|\gamma_i(\tau_{3i}) = 1|$) a superposition of three useful Doppler signals at frequencies is formed at the output of the photodetector

$$\omega_{\lambda 1} = \Omega_M + 8\pi/\lambda_1 \left[\cos\left(\frac{\gamma_1 + \alpha}{4}\right) * \sin\left(\frac{\gamma_1 - \alpha}{4}\right) \right] V_x, \quad (1)$$

$$\omega_{\lambda 2} = \Omega_M + 8\pi/\lambda_2 \left[\cos\left(\frac{\gamma_2 + \alpha}{4}\right) * \sin\left(\frac{\gamma_2 - \alpha}{4}\right) \right] V_x, \quad (2)$$

$$\omega_{\lambda 3} = \Omega_M + 8\pi/\lambda_3 \left[\cos\left(\frac{\gamma_3 + \alpha}{4}\right) * \sin\left(\frac{\gamma_3 - \alpha}{4}\right) \right] V_x, \quad (3)$$

And high-frequency interference signals are automatically suppressed due to the appropriate manifestation of coherence effects. These three useful signals have the same frequency

$$\omega_{\lambda 1} = \omega_{\lambda 2} = \omega_{\lambda 3} = \dots = \omega_{\lambda n},$$

if the geometry of the probing and scattered beams is chosen such that the following relationship is fulfilled

$$\gamma_i = 2 \arcsin\left[\left(\frac{\lambda_i}{\lambda_1}\right) \sin\frac{\gamma_1}{2} + \left(\frac{\lambda_1 - \lambda_i}{\lambda_1}\right) \sin\frac{\alpha}{2}\right], \quad (4)$$

where $i=2, 3, \dots, n$,

α - reception angle between two scattered beams 33 and 34;

γ_1 - the angle between the probing beams at the wavelength λ_1 .

Useful Doppler signals (1), (2) and (3) have the same frequencies, proportional to the horizontal velocity projection $V_x = V_{\cos \varphi}$, however, effective reception is achieved by ensuring that these signals are in phase [3] with the help of phase regulators 23 and 25. The signal from the output of the photodetector 40 enters the input of the Doppler frequency meter 41, which outputs information about the module and the speed projection $\text{sign} \pm V_z$.

The developed scheme of the BLDA allows to significantly increase the signal-to-noise ratio, range and measurement accuracy, due to the use of n-number of lasers emitting at different wavelengths of electromagnetic radiation, including infrared radiation, as well as such a geometry of multi-wavelength probing and reception of scattered radiation, in which the frequencies of the Doppler signal do not depend on the wavelength of the laser radiation, which allows for in-phase coherent reception of optical signals, while simultaneously suppressing high-frequency interference.

The field of application of BLDA extends to high speeds, for example, hypersonic aerodynamic flows, in which there are no large microparticles ($dz < 0.1 \mu\text{m}$).

References

1. July 2, 1982 - by the date of registration of application No. 3463808 for the invention "Diferentiall laser anemometer" in the State Inventor of the USSR
2. Laser anemometry, remote spectroscopy and interferometry: Handbook/Ed. M.S. Pacifier - K.: Naukova Dumka, 1985.-759p.
3. Zemlyansky V.N. Measurement of the velocity of laser flows by the Doppler method. - K.: Vyshcha Shk., 1987. - 177p.
4. Multi-wavelength laser Doppler anemometer. Zemlyansky V.M., Gusev M.O., Lobzov K.A. Application to UkrPatent for invention No. 202203184 dated September 1, 2022